



**Self-assembly Nanostructured Gold for High Aspect Ratio  
Silicon Microstructures By Metal Assisted Chemical Etching**

Journal:	<i>RSC Advances</i>
Manuscript ID	RA-COM-11-2015-024947.R1
Article Type:	Communication
Date Submitted by the Author:	20-Jan-2016
Complete List of Authors:	Romano, Lucia; Dipartimento di Fisica e Astronomia, Università di Catania; IMM-CNR University of Catania; Swiss Light Source, Paul Scherrer Institut Kagias, Matias; Swiss Light Source, Paul Scherrer Institut; Institute for Biomedical Engineering, University and ETH Zürich Jefimovs, Konstantins ; Swiss Light Source, Paul Scherrer Institut; Institute for Biomedical Engineering, University and ETH Zürich Stampanoni, Marco; Swiss Light Source, Paul Scherrer Institut; Institute for Biomedical Engineering, University and ETH Zürich
Subject area & keyword:	Nanomaterials - Materials < Materials



## COMMUNICATION

## Self-assembly Nanostructured Gold for High Aspect Ratio Silicon Microstructures By Metal Assisted Chemical Etching

Received 00th January 20xx,  
Accepted 00th January 20xx

L. Romano,<sup>a,b\*</sup> M. Kagias,<sup>b,c</sup> K. Jefimovs<sup>b,c</sup> and M. Stampanoni<sup>b,c</sup>

DOI: 10.1039/x0xx00000x

[www.rsc.org/](http://www.rsc.org/)

**Self-assembly gold nanostructured membranes are created to mechanically stabilize the catalyst movement during metal assisted chemical etching. This results into an improved vertical control of the etching profile for high aspect ratio silicon microstructures. The new method is a robust and cheap microfabrication for dense micro-patterns on large area, such as diffraction gratings for hard X-ray phase contrast imaging and metrology.<sup>1</sup>**

Metal-assisted chemical etching (MACE) is an electro less chemical etching technique that can etch high aspect ratio micro – nanometer sized features in silicon substrates.<sup>2-4</sup> MACE is reported as a simple and cost efficient method used to fabricate nanoporous silicon,<sup>2,3</sup> high aspect ratio Si nanowires,<sup>4</sup> and nanostructures.<sup>5-11</sup> In MACE, a metal layer (e.g. Au) is patterned onto the substrate (e.g. Si) to locally increase the dissolution rate of the substrate material in an etchant solution of hydrofluoric acid (HF) and an oxidizing agent such as hydrogen peroxide (H<sub>2</sub>O<sub>2</sub>).<sup>4</sup> The Au is used as a

preferential catalyst for Si high aspect ratio structures because it is chemically stable, it does not oxidize and it has one of the fastest etching rates.<sup>4</sup> The H<sub>2</sub>O<sub>2</sub> is reduced at the Au surface producing water and at the same time injecting holes through the Au catalyst into Si.<sup>2,4</sup> At the Au–Si interface, the Si atoms underneath the Au catalyst are oxidized by the holes and dissolved in the HF solution as H<sub>2</sub>SiF<sub>6</sub>.<sup>4</sup> Since there are hole-injection and Si dissolution processes, mass transfer is one of the key factors in the etching process. In addition, H<sup>+</sup> ions and hydrogen gas (H<sub>2</sub>) are produced as byproducts of the reaction.<sup>4</sup> Unlike KOH wet etching,<sup>12</sup> the MACE process is independent of crystal orientation under most conditions and may be used to create a wide variety of hole profiles, trenches, morphologies and paths.<sup>10</sup> In comparison to other high- aspect ratio micromachining techniques,<sup>13</sup> MACE processing area is not limited by the equipment in use, nonetheless scalability can be achieved at a relatively low cost.

<sup>a</sup> Department of Physics and CNR-IMM- University of Catania, 64 via S. Sofia, Catania, I-95023, Italy. [luca.romano@ct.infn.it](mailto:luca.romano@ct.infn.it)

<sup>b</sup> Swiss Light Source, Paul Scherrer Institut, Villigen PSI, 5232, Switzerland.

<sup>c</sup> Institute for Biomedical Engineering, University and ETH Zürich, Zürich, 8092, Switzerland.

†Electronic Supplementary Information (ESI) available: details of any supplementary information available should be included here. See DOI: 10.1039/x0xx00000x

MACE resulted to be very efficient for massive production of Silicon nanostructures,<sup>4-9</sup> nanowires and ordered nanopillars. On the other hand etching of microscale patterns of arbitrary shape and density is more critical regarding the control of etching depth and direction.<sup>14</sup> Hildreth et al.<sup>10,11</sup> demonstrated that for metal isolated nanopatterns (nanodots, nanodonuts, nanolines, grids, squares, discs etc.)<sup>10</sup> the etching direction into the Si is intimately related to the geometry of the catalysts and the local charge carriers distribution. Controlled 3D motion of catalyst patterns during MACE can be achieved by locally pinning them with an electrically insulating material prior to etching.<sup>11</sup> However, due to this movement, the maximum achievable aspect ratio for vertical features in an arbitrary dense pattern is limited.<sup>4</sup> Vertical directionality controlled MACE has been reported for patterning X-ray diffractive optics with nanoscale periods on hundreds square micrometers area by using bridged catalytic structures, which improve mechanical stability of pattern, and additional surrounding metal patterns serving as holes concentration balancing structures.<sup>15</sup> Etching in the microscale regime is more critical, the etching rate is limited by the reactant diffusion through the metal mask. The effective transfer of reactants and their by-products would not be identical where the metal pattern size is nanometers or few micrometers. Porous catalyst film is reported<sup>14, 16</sup> to improve the etching performances of micro-scaled Si trenches interdigitated structures of few micrometer feature size and the length in the range of few hundreds micrometers.<sup>14</sup> However, the morphology of catalyst film was not deeply investigated and well controlled. In this paper, we present a novel approach for controlling the vertical directionality and substantially improving the stabilization of the MACE processing for etching patterns of different sizes on large area (4 inch wafer), without the need of any supporting structures<sup>11, 15</sup> or magnetic

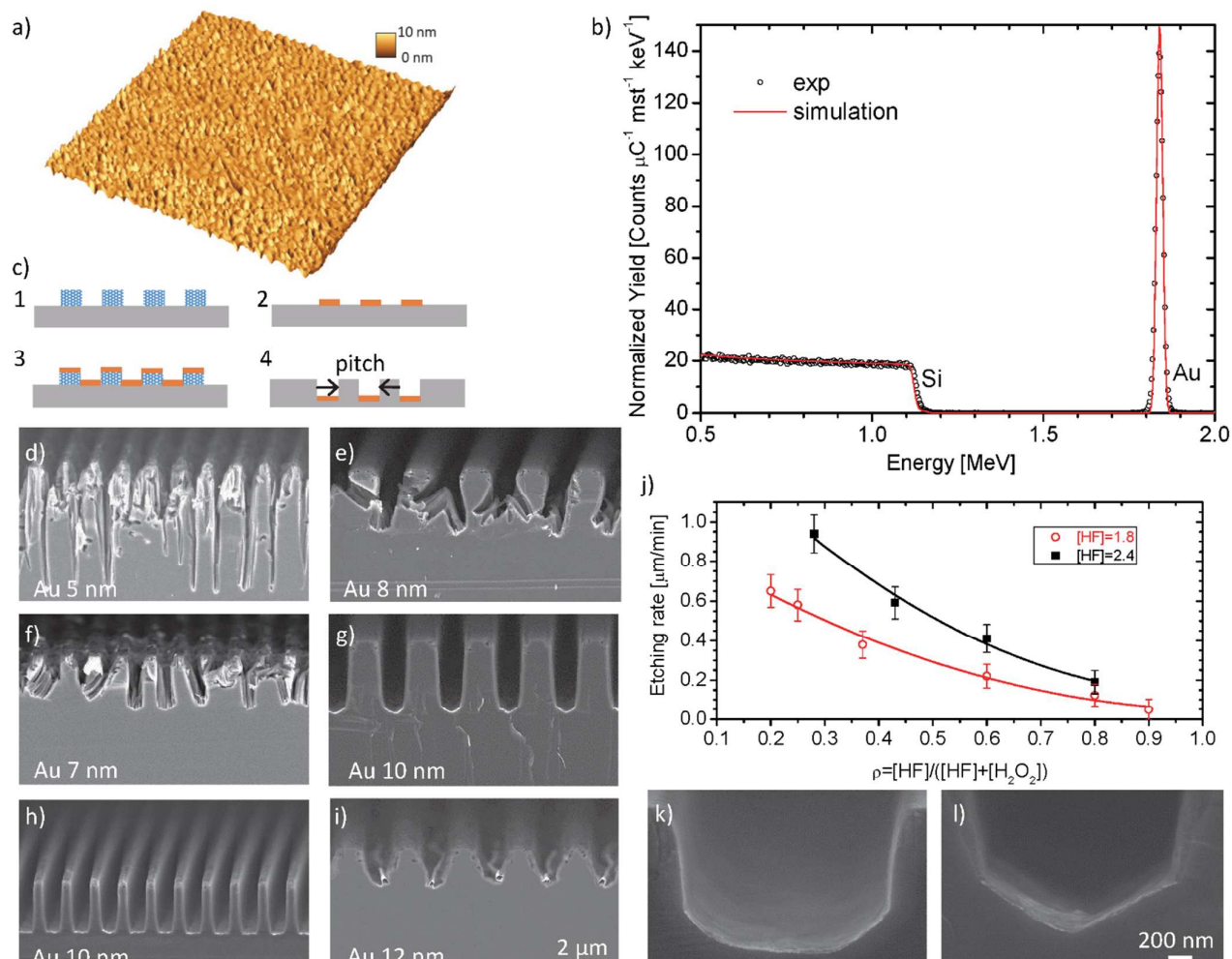


Figure 1. As deposited 10 nm Au film characterizations: (a) AFM  $1 \mu\text{m} \times 1 \mu\text{m}$  scan; (b) 2 MeV  ${}^4\text{He}^+$  RBS spectrum, Si and Au signal are indicated, the spectrum is fitted<sup>27</sup> with  $6.4 \times 10^{16} \text{ Au/cm}^2$  corresponding to  $10 \pm 1 \text{ nm}$  Au film on bulk Si; (c) Schematic of the microfabrication process: 1) a sacrificial photoresist pattern was formed on Si substrate by conventional photolithographic methods; 2) the substrate is cleaned with Oxygen plasma to form an Oxygen-terminated Si surface and a thin film of Au is subsequently deposited on Si; 3) lift-off in the proper solvent leaves the Au pattern on the substrate and removes the photoresist; 4) MACE by dipping the substrate in an etching solution that contains HF and  $\text{H}_2\text{O}_2$ , resulting into a Au pattern that sinks in the Si substrate SEM cross-view of grating with pitch of  $2.4 \mu\text{m}$  (d, f, h) and  $4.8 \mu\text{m}$  (e, g, i) and different Au film thickness: 5 nm (d), 8 nm (e), 7 nm (f), 10 nm (h, g), 12 nm (i). Figures e, f, g, h and i have the same marker, showed in figure i; (j) Etching rate of gratings with  $4.8 \mu\text{m}$  pitch and 10 nm Au film. SEM cross-view of Si grooves etched with HF- $\text{H}_2\text{O}_2$ - $\text{H}_2\text{O}$  solution ( $\rho=0.2$ ,  $[\text{HF}]=1.8 \text{ mol/l}$ ) after 2 min (k), 10 (l). Figures k and l have the same marker, showed in figure l.

catalyst.<sup>17</sup> By studying the morphology and the evolution of gold film at different MACE conditions, we found that the detrimental catalyst movement is substantially reduced by inducing a self-assembly nanostructuring of the metal film. For this purpose, we used the property of thermally induced Au de-wetting on an oxygen terminated silicon surface.<sup>18</sup> We demonstrated uniform large area dense patterns, which makes MACE a reliable fabrication method in the microscale range. Figure 1 reports the morphology and etching study of the Au film deposited on top of Si substrate. Experimental details are reported in ESI<sup>†</sup>. Since the film morphology strictly depends on the deposition parameters (deposition rate, temperature and deposition methods, such as evaporation by electron beam, thermally induced evaporation, sputtering etc),<sup>18</sup> this preliminary study was useful to establish the optimal film morphology. Fig. 1a shows the typical granular morphology of a

thin Au film with small Au clusters in the nanometer range, the reactant diffusion of the etching solution occurs at the edge of these nanoparticles. First, we characterized the Au film morphology by using several surface techniques: Atomic Force Microscopy (AFM) and Scanning Electron Microscopy (SEM) were used to study the 2D-3D morphology of the Au films, while Rutherford Backscattering Spectrometry (RBS) allows measuring the full amount of Au per surface area deposited on the substrate. By combining the information of these three characterizations, it is possible to obtain a complete description of the Au morphology. For example, for Au film thickness of 10 nm, the concentration of Au surface atoms is about  $6.4 \times 10^{16} \text{ Au/cm}^2$  (simulation of the experimental data is reported in Fig. 1b), the Au clusters are very close packed with size is in the range of 1-12 nm and roughness of 1 nm. Second, a grating pattern was formed according to the schematic of

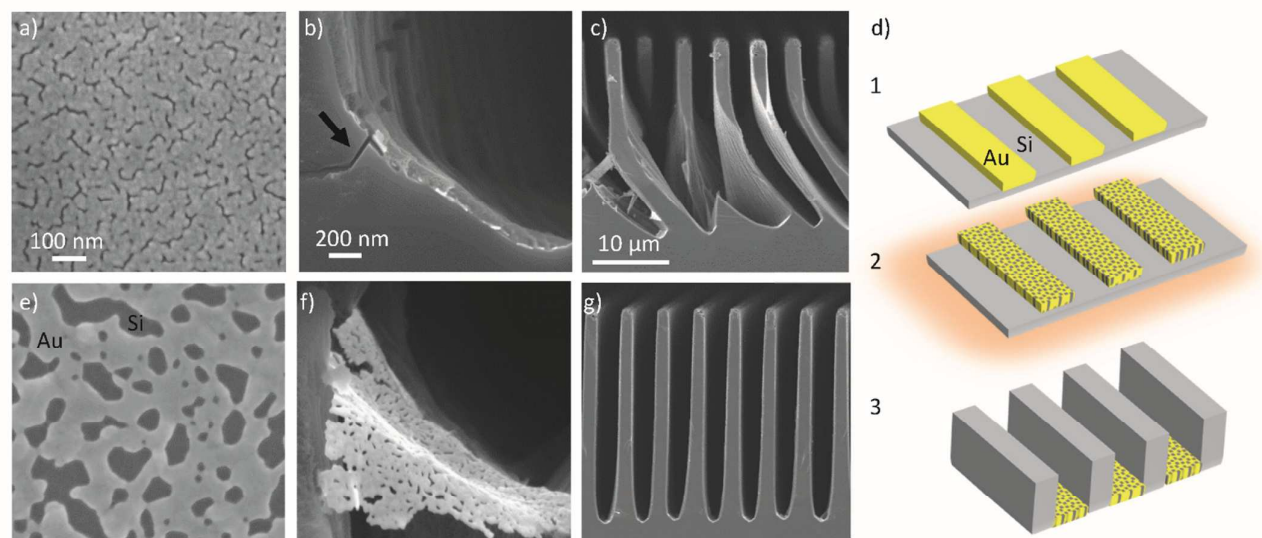


Figure 2. SEM planar-view of as-deposited 10 nm Au (a); SEM cross-view of Si grooves etched with HF-H<sub>2</sub>O<sub>2</sub>-H<sub>2</sub>O solution ( $\rho=0.2$ , [HF]=1.8 mol/l) after 15 min (b), and 40 min (c). The arrow (b) indicates a random path created by a detached Au particle that starts the catalyst instability. (d) Schematic of the process for creating interconnected metal membrane that mechanically stabilize the Au catalyst during MACE: 1) gold pattern realized by lithography and Au thin film deposition; 2) thermal treatment to induce Au dewetting; 3) MACE. SEM planar-view (e) of de-wetted Au film annealed at 250°C for 30 min (75% Au coverage, the bright signal is Au, the darker is Si); SEM cross view of grating after 40 min etching ( $\rho=0.2$ , [HF]=1.8 mol/l): a piece of metal membrane (f), the grating with metal membrane (g) that prevents the undercut and preserves the vertical directionality of MACE. Figures a, b, c, d, e, f and g have the same marker, showed in figure c.

Fig. 1c: 1) a sacrificial photoresist pattern was formed on Si substrate by conventional UV photolithography; 2) the substrate was cleaned with Oxygen plasma to form an Oxygen-terminated Si surface and a thin film of Au is subsequently deposited on Si; 3) lift-off in the proper solvent leaved the Au pattern on the substrate and removed the photoresist; 4) MACE by dipping the substrate in an etching solution that contains HF and H<sub>2</sub>O<sub>2</sub>, results into a Au pattern that sinks in the Si substrate. As the Au catalyst moves down to occupy the space vacated by the etched Si, the substrate is carved into shapes defined by the shapes of the catalyst pater. We assume that the main driving force of this mechanism is the Si-catalyst attraction due to van der Waal's force.<sup>19</sup> The film thickness of the deposited Au was varied in the range of 5-12 nm and the effect on MACE features is reported in the sequence of Fig. 1d-i. MACE's performance is highly sensitive to the Au film thickness: when the Au film is too thin (Fig. 1d-f), the etching is very fast and not uniform (Fig. 1d) or very unstable (Fig. 1e-f) and the grating pattern is not vertically transferred to Si, since the catalyst acts like an ensemble of nanoparticles which suffer of catalyst random movement during the etching process. Au film thickness of 10 nm resulted into a clustered morphology that allows a slower etching and a good diffusion of the etchants through the catalyst, with the consequent vertical etching (Fig. 1h and 1g). With increasing Au thickness, the interstitial space within the Au clusters is not enough (e.g. the porosity of the film is not sufficient) and the diffusion of chemical reactants through the catalyst film is limited. In this condition, the etchants must travel back and forth beneath the Au layer to dissolve the Si and get byproducts out. As a consequence, the etching proceeds faster

at the edge of the Au film leading to a final bending of the Au lines from the edges towards the center,<sup>16</sup> which finally compromises the vertical directionality of the etched pattern (Fig. 1i). Once the film morphology is fixed, the etching rate depends on the relative ratio between the concentration of the etchants, HF and H<sub>2</sub>O<sub>2</sub>:  $\rho = \text{HF}/(\text{HF} + \text{H}_2\text{O}_2)$ , where HF and H<sub>2</sub>O<sub>2</sub> are the concentrations of HF and H<sub>2</sub>O<sub>2</sub>, respectively, in moles per liter.<sup>3</sup> Fig. 1j reports the typical etching rate obtained for a grating structure (pitch 4,8 μm) with 10 nm thick Au patterning. The evolution of the catalyst film was observed as a function of the etching time for several etching conditions. Fig. 1k and 1l show the cross section of the bottom of the Si grooves that are formed because the Au catalyst penetrates the Si substrate, while the etching solution oxidizes and removes Si underneath Au. During etching the Au film changes its shape: initially the Au film remained flat (Fig. 1k), then it progressively bent (Fig. 1l), forming a convex angle relative to the surface normal as the etching proceeded. The time for developing this convex shape depends on the etching rate but this particular shape was observed for all the etching conditions. The convex shape indicated that the etching is faster in the center of the Au line, according with the fact that the peak of the injected holes is at the Si-Au interface.<sup>20</sup> Therefore, the process is dominated by the charge transport, since the reactant transport is provided through the pores of the catalyst film.<sup>16</sup> However, the achievable etching depth is limited at a critical value of about 10 μm. Our study suggests that instability and catalyst movement are the main reasons for limiting the fabrication of high-aspect ratio Si micro-patterns.

Figure 2 reports the experimental observations of the critical etching caused by a catalyst instability and the proposed solution. Since the morphology of the film catalyst is granular and the Au clusters are physically separated (Fig. 2a) from each other, some particles get detached from the film and continued etching in a random direction (Fig. 2b). The catalyst instability started with the loss of some Au nanoparticles that left the main Au film as the catalyst progressively sank into Si. As the etching proceeded, pushing the catalyst further inside the Si substrate, the detrimental catalyst movement compromises the verticality of the etching. As a consequence, the etching followed random directions with a deviation from the initial vertical axis. The reported splaying effect occurred,<sup>15</sup> with a dramatic undercutting of the grating lines (Fig. 2c). The catalyst instability is favoured by the H<sub>2</sub> gas formation as byproduct of the etching chemical reaction.<sup>2</sup> Since gas bubbles were observed during the etching process, a strong pressure should be present at the Au-Si interface. Therefore, the Au thin film is subjected to an additional mechanical stress, which can be responsible of the breaking of the continuous pattern. The mechanical instability is prevented by introducing a process to reinforce the Au film prior the MACE, Fig. 2d shows a schematic of this approach. A thermal treatment induced Au de-wetting on Oxygen-terminated Si surface,<sup>18</sup> this increased the porosity of the catalyst film and strengthened the metal network. Fig. 2e

shows the new metal interconnected structure as it is formed on Si substrate after annealing at 250°C for 30 minutes in air, the Au coverage is about 75%. In contrast to thin film deposition, where film porosity depends on various deposition parameters (substrate temperature, deposition rate, film thickness and deposition method), the porosity of de-wetted Au can be finely tuned as a function of the annealing temperature and the film thickness.<sup>18</sup> No Au alloy formation is reported for annealing of Au on SiO<sub>2</sub> at temperature below 800°C,<sup>21</sup> so at low temperature the metal film experienced a physical rearrangement that changes its morphology without diffusing deeper in the substrate. The new metal interconnected structure looks like a membrane and is much more stable during the MACE process, it can be bent without losing its membrane shape. Fig. 2f shows a piece of the metal membrane after traveling for 30 μm into Si during a long etching process. The self-assembly metal membrane allows to obtain deep Si grooves with a relevant vertical directionality control (Fig. 2g), in comparison to uncontrolled undercut structures realized without membrane in the same etching conditions (Fig. 2c).

H<sub>2</sub> gas release during MACE not only affects the mechanical stability of the catalyst pattern but also fosters non-uniform etching. Optical microscopy detected several circular regions of hundreds of micrometers in size where the etching depth was reduced by a few μm with respect of surrounding regions. The etching uniformity was improved by adding a surfactant, such as Isopropanol alcohol (IPA), which promotes the release of smaller bubbles in the HF-H<sub>2</sub>O<sub>2</sub>-H<sub>2</sub>O solution. We observed a visible reduction of bubbles size in the etching solution by adding few ml of IPA. IPA has also the benefit<sup>22</sup> to reduce the silicon roughness in HF-H<sub>2</sub>O<sub>2</sub> solution by substantially improving the inherent Si microporosity of MACE.<sup>3,4</sup> Figure 3 shows the cross-section SEM of 4 inches grating with Si grooves 40 μm (Fig. 3a) and 80 μm-deep (Fig. 3b), the aspect ratio is 20:1 and 40:1, respectively. With the exception of the perimetric pattern, the etching depth has a variation of 1.5 μm over 40 μm, i.e. less than 5% over the entire 4 inch wafer (Fig. 3c).

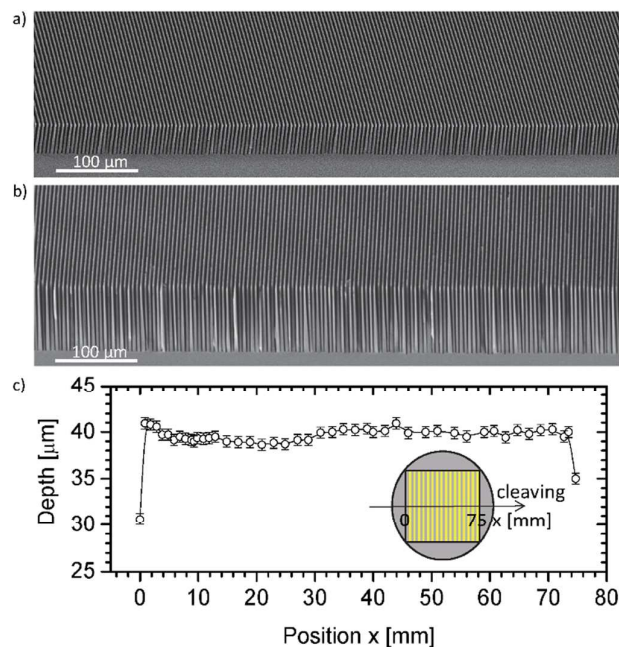


Figure 3. (a) 40 μm (aspect ratio 20:1) and (b) 80 μm (aspect ratio 40:1) deep Si gratings with Au metal membranes from 10 nm Au film annealed at 180°C for 30 min (86% Au coverage) and etched at  $p=0.6$ ,  $[HF]=3.5$  mol/l with the addition of IPA in order to promote the H<sub>2</sub> gas release in small bubbles during MACE. Figures a and b have the same marker, showed in figure a. (c) Etching uniformity of the 40 μm deep grating, the Si depth is measured in high resolution SEM images (not-shown) collected in several regions over the cleaving direction indicated in the insert (schematic of the metal pattern on 4 inches Si wafer).

## Conclusions

We reported on the peculiar effect of Au catalyst morphology on the etching performance of MACE, where catalyst instabilities are responsible of limiting aspect ratio in microscale Si dense patterns. We demonstrated an improved mechanical stability of the metal film by nanostructuring the Au layer through a self-assembly mechanism of de-wetting. Controlled porosity of the catalyst was required for etching pattern of different size in the microscale regime. A straight forward and tunable self-assembly of the Au film on top of Oxygen-terminated Si surface was realized by a thermal treatment at low temperature (>100°C). The new membrane catalyst is mechanically more stable than a clustered Au film and avoids the detrimental catalyst movement during the etching process. Nanostructured self-assembly Au membrane and controlled gas release with the addition of IPA to the

etching solution were finally optimized for producing high directional - high aspect-ratio Si micro-structures on large scale by MACE. This new strategy has no limitation in the large-area application since the etching is performed in a liquid phase. A considerable reduction in fabrication costs and complexity are characteristic of the method. Nonetheless accessibility even in labs with limited equipment (no vacuum or clean-room conditions) promotes wide applicability of MACE in various applications wherever micro-machining is required, for example high aspect ratio gratings for X-ray grating interferometry,<sup>1</sup> MEMS,<sup>14</sup> sensors,<sup>23</sup> photonic devices,<sup>24</sup> thermoelectric materials,<sup>25</sup> and battery anodes.<sup>26</sup>

### Acknowledgements

This work has been partially funded by the ERC-2012-STG 310005-PhaseX grant and the Fondazione Araldi Guinetti. C. David (PSI) and A. Sakdinawat (SLAC) for fruitful discussions; S. Tatì (CNR-IMM, University of Catania) and D. Marty (PSI-LMN) for technical support.

### Notes and references

- 1 T. Weitkamp, A. Diaz, C. David, F. Pfeiffer, M. Stampanoni, P. Cloetens, and E. Ziegler, *Opt. Express* 2005, **13**, 6296.
- 2 X. Li and P. W. Bohn, *Appl. Phys. Lett.* 2000, **77**, 2572.
- 3 C. Chartier, S. Bastide, C. Lévy-Clément, *Electrochim. Acta* 2008, **53**, 5509.
- 4 Z. Huang, N. Geyer, P. Werner, J. D. Boor, U. Gösele, *Adv. Mater.* 2010, **23**, 285.
- 5 H. Hana, Z. Huang, W. Lee, *Nano Today* 2014, **9**, 271.
- 6 K. Q. Peng, J. J. Hu, Y. J. Yan, Y. Wu, H. Fang, Y. Xu, S. T. Lee and J. Zhu, *Adv. Funct. Mater.* 2006, **16**, 387.
- 7 M. Bechelany, E. Berodier, X. Maeder, S. Schmitt, J. Michler, and L. Philippe, *ACS Appl. Mat. Interfaces* 2011, **3**, 3866.
- 8 X. Liu, *Curr. Opin. Solid State Mater. Sci.* 2012, **16**, 71.
- 9 X. Liu, P. R. Coxon, M. Peters, B. Hoex, J. M. Cole and D. J. Fray, *Energy Environ. Sci.* 2014, **7**, 3223.
- 10 O. J. Hildreth, W. Lin, C. P. Wong, *ACS Nano* 2009, **3**, 4033.
- 11 K. Rykaczewski, O. Hildreth, C. P. Wong, A. Fedorov, *Adv. Mater.* 2010, **23**, 659; O. J. Hildreth, D. Brown and C. P. Wong, *Adv. Funct. Mater.* 2011, **21**, 3119; O. J. Hildreth, K. Rykaczewski, A. G. Fedorov, and C. P. Wong, *Nanoscale* 2013, **5**, 961.
- 12 B. Wu, A. Kumar, and S. Pamarthy, *J. Appl. Phys.* 2010, **108**, 051101.
- 13 V. Saile, *LIGA and its Applications*, in *Advanced Micro and Nanosystems*, Vol. 7 (Eds: V. Saile, U. Wallrabe, O. Tabata and J.G. Korvink) Wiley-VCH, Weinheim, Germany 2009, Ch. 1.
- 14 M. Zahedinejad, S. D. Farimani, M. Khaje, H. Mehrara, A. Erfanian, and F. Zeinali, *J. Micromech. Microeng.* 2013, **23**, 055015.
- 15 C. Chang and A. Sakdinawat, *Nat. Commun.* 2014, **5**, 4243.
- 16 L. Li, Y. Liu, X. Zhao, Z. Lin, and C. Wong, *ACS Appl. Mat. Interfaces* 2014, **6**, 575.
- 17 Y. Oh, C. Choi, D. Hong, S. D. Kong, and S. Jin, *Nano Lett.* 2012, **12**, 2045.
- 18 C.V. Thompson, *Annu. Rev. Mater. Res.* 2012, **42**, 399.
- 19 C.Q. Lai, H. Cheng, W.K. Choi and C. V. Thompson, *J. Phys. Chem. C* 2013, **117**, 20802.
- 20 P. Lianto, S. Yu, J. Wu, C. V. Thompson, and W. K. Choi, *Nanoscale* 2012, **4**, 7532.
- 21 J.F Chang, T.F Young, Y.L Yang, H.Y Ueng, T.C Chang, *Mater. Chem. Phys.* 2004, **83**, 199.
- 22 D.H. Eom, K.S. Kim and J.G. Park, *Jpn. J. Appl. Phys.* 2002, **41**, 5881.
- 23 S. M. Sze, *Semiconductor Sensors*, Wiley, New York, USA 1994
- 24 K. Balasundaram, P. K. Mohseni, Y.-C. Shuai, D. Zhao, W. Zhou, and X. Li, *Appl. Phys. Lett.* 2013, **103**, 214103.
- 25 G. J. Snyder, J. R. Lim, C.K. Huang, and J.P. Fleurial, *Nature Materials* 2003, **2**, 528
- 26 M. R. Zamfir, H. T. Nguyen, E. Moyon, Y. H. Lee and Didier Pribat, *J. Mater. Chem. A* 2013, **1**, 9566
- 27 M. Thompson, RUMP: Rutherford backscattering spectroscopy analysis package, <http://www.genplot.com>, accessed: September, 2015.

## Self-assembly Nanostructured Gold for High Aspect Ratio Silicon Microstructures By Metal Assisted Chemical Etching

Lucia Romano\*, Matias Kagias, Konstantins Jefimovs, Marco Stampanoni

Textual abstract

Self-assembly gold nanostructured membranes are created to mechanically stabilize the catalyst movement during metal assisted chemical etching, resulting into an improved vertical control of the etching profile for high aspect ratio silicon microstructures. The new method results into a robust and cheap microfabrication capable for dense micro-patterns on large area, such as diffraction gratings for hard X-ray phase contrast imaging and metrology.

Graphical abstract

